

Photoionization of endohedral molecules: $N_2@C_{60}$

P. Decleva¹ and S. T. Manson^{2*}

¹Istituto Officina dei Materiali IOM-CNR and Dipartimento di Scienze Chimiche e Farmaceutiche, Università di Trieste, Via Giorgieri 1, I-34127 Trieste, Italy

²Department of Physics and Astronomy, Georgia State University, Atlanta, GA 30303, USA

Abstract

Calculations of the photoionization of the nitrogen $1\sigma_g$, $1\sigma_u$, and $2\sigma_g$, states of the $N_2@C_{60}$ molecule are performed at the density functional theory (DFT) level taking full account of the molecular geometry of both N_2 and the C_{60} . The results show that cross sections are sensitive to the parity of the final channels, with a complex interplay between the native σ_u resonance in free N_2 and confinement resonances. A quite different behavior is obtained for the asymmetry parameters.

I. Introduction

The capability of the C_{60} cage to encapsulate atoms [1-5] and, more recently, small molecules [6-11] gives rise to a new class of systems with fascinating characteristics, still largely unexplored. For relatively small systems the interaction between the C_{60} cage and the guest is relatively weak. For instance, noble gases are not fixed at the center, as might be reasonably guessed, but oscillate relatively freely within the cage. Still the enclosure modifies profoundly the physical properties, as in first approximation the guest system can be considered as constrained by a spherical potential well, the simplest example of confined systems. The initial preparation of endohedral compounds employed drastic conditions that could be sustained only by atomic systems [1]. More recently it has been possible to encapsulate small molecules employing much more delicate chemical reactions, opening a hole in the cage, inserting the guest, and closing the hole back, a true “chemical surgery” [6-11].

Although properties of encapsulated atoms have been studied quite extensively [3-5], often employing a spherical potential model to simulate the C_{60} cage, very little has been done about confined molecules. With atoms, photoionization from inner shells, that can be clearly distinguished on energetic grounds, have been extensively studied. Since the bound state wave functions of inner shells are completely unaffected by the confining cage, examination of the photoionization of these inner shells amounts to spectroscopy of the final continuum state of the confined atom. The most dramatic phenomena are the appearance of a series of sharp, regular resonances starting at the subshell threshold that are induced by the cage; these are termed confinement resonances [12]. These have been difficult to observe experimentally but have been seen for $Xe@C_{60}$ [13, 14], as they are significantly damped by nuclear motion, not considered in the simulations. The origin of confinement resonance is a purely quantum mechanical coherent

1
2
3 interference between a photoelectron emitted directly and one that undergoes one (or more)
4 reflections from the confining potential before emerging.
5

6 In this work we have undertaken a first exploration considering the N_2 molecule encapsulated in
7 C_{60} , looking at the photoionization of the core N $1s$ orbitals and the inner valence $2\sigma_g$, as these
8 should be, in principle, accessible and well separated in energy from the C_{60} ionization bands.
9

10 Actually in free N_2 the tiny splitting of the $1\sigma_g$ and $1\sigma_u$ orbitals can be resolved [15] and
11 illustrates several interesting features. One is the presence of a strong shape resonance in the $1\sigma_g$
12 channel, due to the strong dipole transition to a molecular virtual level of σ_u character, the
13 antibonding $3\sigma_u$ orbital in the LCAO picture [16, 17]. Another is the presence of weak but clear
14 Cohen-Fano oscillations [18] on a large energy scale, which are traced to interference between
15 electron waves coherently emitted by the two equivalent centers. Actually such oscillations occur
16 in antiphase for the $1\sigma_g$ and $1\sigma_u$ channels, because of the different parities of their corresponding
17 photoelectron waves, and are easily detected experimentally in the $1\sigma_g/1\sigma_u$ cross section ratio. It
18 will not be likely possible to detect such features for $N_2@C_{60}$, due to the broadening of the peaks
19 associated with nuclear motion, but it is still theoretically interesting and informative to follow
20 the modifications of the two separate channels induced by the cage.
21
22
23
24

25 Alternatively, the $2\sigma_g$ molecular orbital in N_2 , although not so strictly localized, bears significant
26 resemblance to the core $1\sigma_g$, and it is of interest to see the extent of cage-induced modifications
27 on the relative photoemission, which have very different ionization energies.
28
29
30

31 **II. Brief theoretical and computational methodology**

32

33 Calculations have been performed at the static-exchange density functional theory (SE-DFT),
34 employing the multicenter B-spline approach [19, 20] with the full molecular potential. The
35 methodology has been extensively detailed [19, 20] and is essentially the same as recently
36 employed in calculation of the free C_{60} molecule [21]. The N_2 molecule, at the free equilibrium
37 distance, has been placed at the center of C_{60} , with its axis parallel to one of the C_5 axes of C_{60} ,
38 reducing the symmetry from I_h to D_{5d} . The one center expansion was defined by a linear grid,
39 with maximum radius $R_{\max}=25$. au and step size 0.25 au, and maximum angular momentum L_{\max}
40 = 30. Radial expansions around the atoms had $R_{\max}=0.40$ au for nitrogen and 1.30 au for carbon,
41 with $L_{\max}=2$. that ensure complete convergence of the calculated parameters.
42
43
44

45 While the geometrical arrangement of maximal symmetry is computationally advantageous, it is
46 not expected that different N_2 orientations within the cage will significantly alter the results, due
47 to the weak interaction between the two subsystems.
48
49
50
51
52
53
54
55
56
57
58
59
60

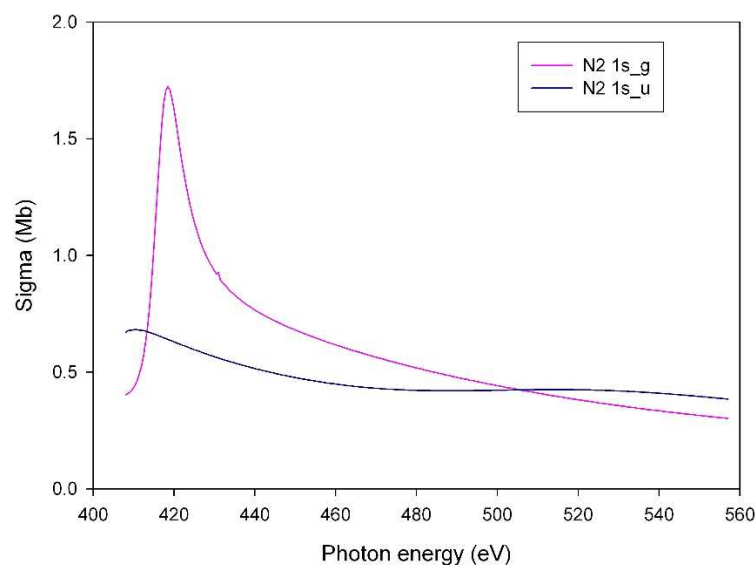


Figure 1. Cross section for the $1\sigma_g$ and $1\sigma_u$ ionization in free N_2

III. Results and discussion

The calculated DFT cross sections for $1\sigma_g$ and $1\sigma_u$ photoionization of free N_2 is shown in figure 1, as a starting point. They are well known [15, 16] and the theoretical results match experiment pretty well [15]. The most conspicuous feature is the strong shape resonance in the $1s_g$ channel discussed above. The calculated $1s$ cross sections of $N_2@C_{60}$ are shown in figure 2, along with the free cross sections for comparison. The confined $1\sigma_g$ spectrum is completely altered with a much stronger and sharper main resonance slightly shifted at higher energy, and a series of smaller resonances; sharp at lower energy and progressively wider at higher energies which are similar to the confinement resonances in atomic endohedral systems [3-5].

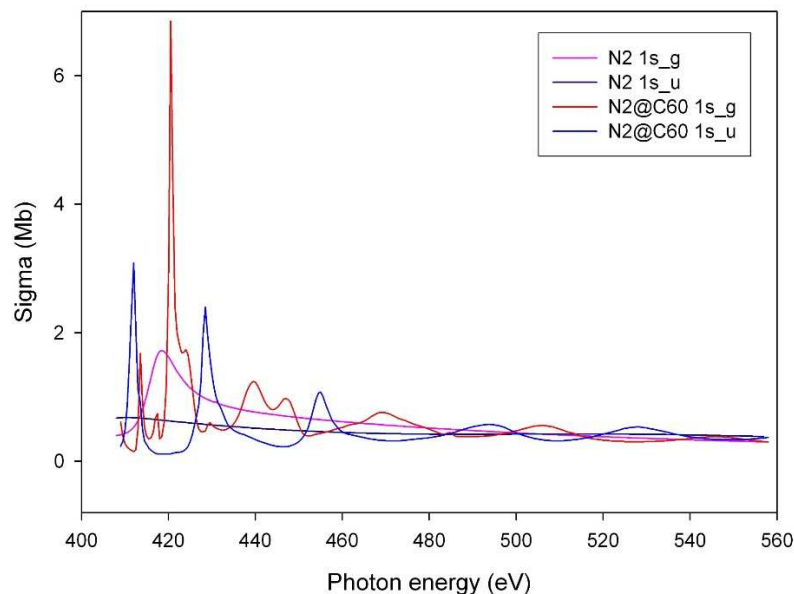


Figure 2. Cross section for the $1\sigma_g$ and $1\sigma_u$ ionization in $N_2@C_{60}$ compared to free N_2 .

An analogous change is present in the $1\sigma_u$ profile, with a more regular series of resonances, sharper at low energy and progressively wider. These are better seen on an enlarged scale in figure 3.

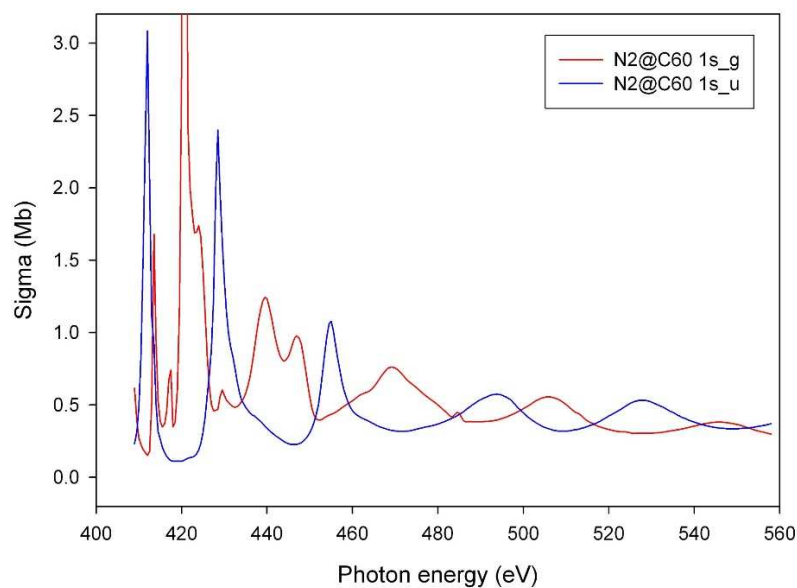


Figure 3. Cross section for the $1\sigma_g$ and $1\sigma_u$ ionization in $N_2@C_{60}$.

Since the $1\sigma_u$ photoionization channel is free of resonances in free N_2 , these resonances in $N_2@C_{60}$ must be induced by the confinement in the cage, i.e., they are typical confinement resonances [12]. The combination of these confinement resonances with the native σ_u shape resonance in the confined $1\sigma_g$ channel gives rise to a more complex feature in that energy range with a kind of splitting into a double peak structure, and some minor peaks in the low energy region. This seems to indicate that the native $1\sigma_g$ shape resonance and the confinement resonances interact coherently, and in a complicated manner, despite former being molecular in origin and the latter being essentially geometrical. Furthermore, this coherence shows that the confinement resonances are a particular class of shapes resonances.

A most interesting feature is the regular interleaving of the resonances, seen clearly in figure 3, and even more clearly in figure 4 where the ratio of the $1\sigma_g/1\sigma_u$ cross sections are displayed. This interleaving is evidently a signature of the different parity of the initial states and that of the corresponding continuum waves, which interact with C_{60} states of the same parity. We expect that this feature is probably universal for all centrosymmetrical systems. Actually it might have been anticipated, as the same occurs for ionization of the outermost ionization in free C_{60} , which show regular out of phase oscillations for initial states of opposite parity, $6h_u$ versus $6g_g, 10h_g$ [21-23]. It might be instructive to see if there is a similar discrimination for other initial symmetries, by investigating confined molecules with different symmetries. In any case, the $1\sigma_g/1\sigma_u$ cross section ratio in figure 4 shows the regular alternation of resonances in σ_g and σ_u channels and gives rise to a very regular series of strong oscillations. On this scale the much weaker Cohen-Fano oscillations are hardly visible and occur on a much wider energy scale [18], e.g., the second Cohen-Fano maximum is at about 480 eV in free N_2 .

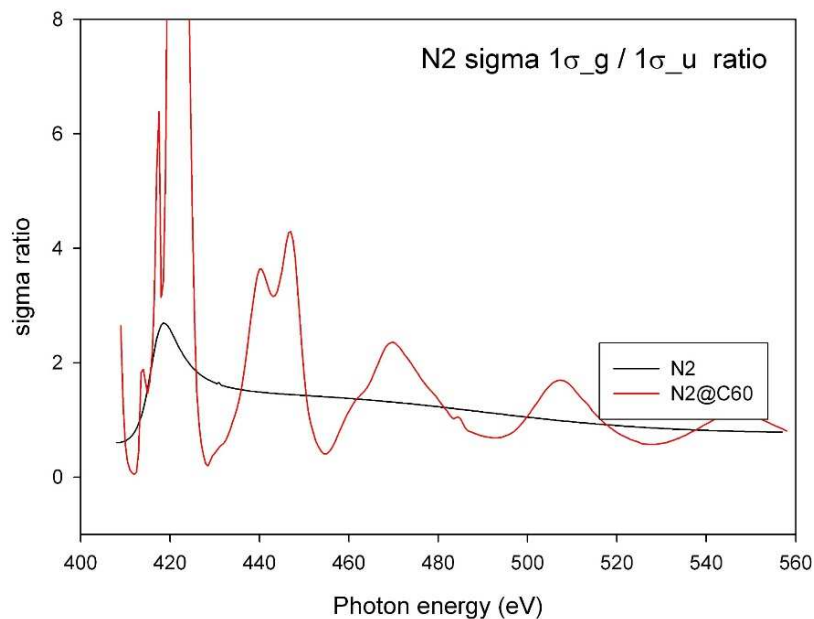


Figure 4. $1\sigma_g/1\sigma_u$ photoionization cross section ratio in $N_2@C_{60}$ along with free N_2 for comparison.

Looking now at the dipole photoelectron angular distribution asymmetry parameter, β , the calculated results for free N_2 are reported in figure 5, where the signature of the σ_u resonance in the $1\sigma_g$ channel is a narrow dip, superimposed on the rapid increase of β towards the asymptotic value of 2. Again this behavior is well known and experimentally verified [16]. A signature of Cohen-Fano oscillations [24] is seen in the very shallow dip of the $1\sigma_u$ β profile around 480 eV.

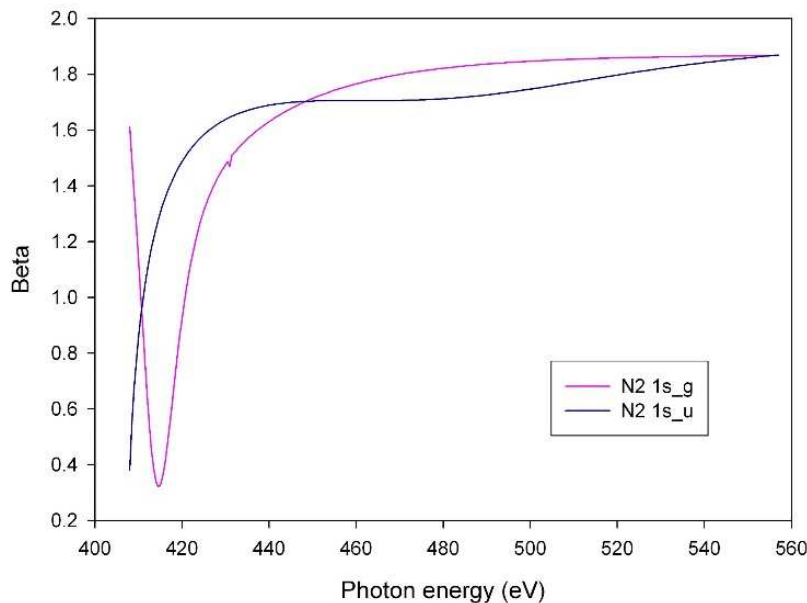


Figure 5. Asymmetry parameter β for $1\sigma_g$ and $1\sigma_u$ photoionization in free N_2 .

The β parameter results for the endohedral system are reported in figure 6; as was the case for the cross sections, the change in the β profile owing to the confinement is dramatic. At variance with the cross section, however, here the gross features of the profile are very similar for both channels; a steep decrease of β towards a very deep minimum, in the negative range, at about 430 eV, (some 20 eV above the σ_u resonance) followed by a gradual increase which remains well below the free N_2 values, even ~ 150 eV above threshold. On this similar pattern a series of very many irregular oscillations, of smaller amplitude, are superimposed, without an obvious connection with the confinement resonances in the cross section. Although the confined cross section of the two $1s$ states are very different, as seen above, this is not the case for the β parameters. Apparently, being a cross section ratio, the asymmetry parameter does not feel strongly the confinement resonances, and therefore the g/u difference. On the other hand the confined β 's are very different from the β parameters for free N_2 , indicating that confinement affects both channels considerably, and in similar ways. However, the origin of the small variations in the β parameters is not clear and might be due to higher angular momentum partial waves that do not materially affect the cross sections.

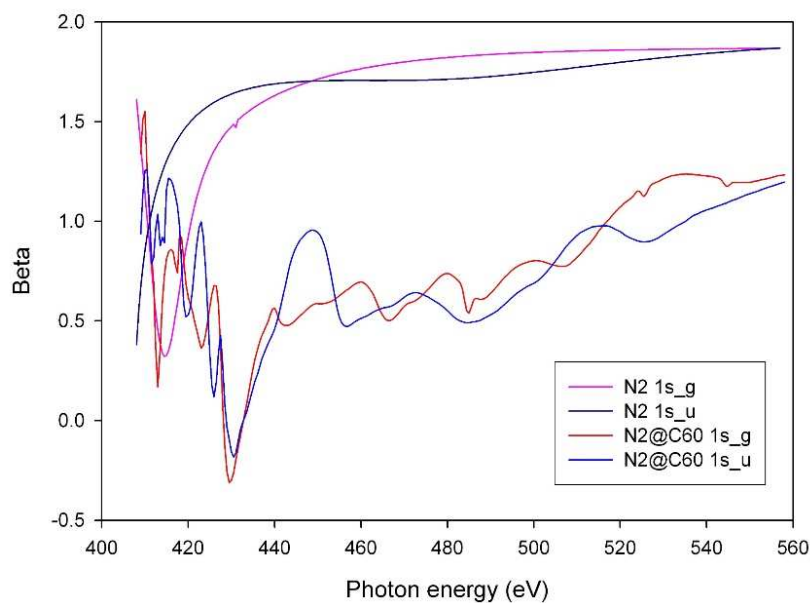


Figure 6. β parameter for the $1\sigma_g$ and $1\sigma_u$ ionization in $N_2@C_{60}$ compared with free N_2 .

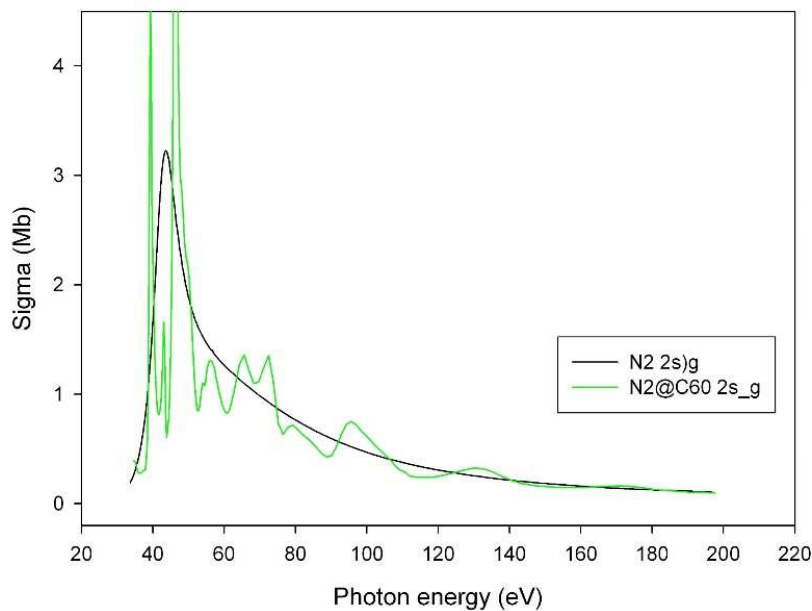


Figure 7. Cross section for the $2\sigma_g$ ionization in $N_2@C_{60}$ compared to free N_2 .

Finally we investigate the photoionization of the inner valence $2\sigma_g$ orbital with the core $1\sigma_g$, and a comparison of the $2\sigma_g$ photoionization cross sections for the free and the endohedral system is

presented in figure 7. Although both the energy and cross section scales are rather different from the core $1\sigma_g$ case, the change engendered by the confinement closely resembles qualitatively what occurs in the $1\sigma_g$ case. The splitting of the $2\sigma_g$ shape resonance in the confined case is particularly striking. The two σ_g cross sections are compared in figure 8, where the resemblance is striking, apart for a curious loss of one oscillation in the 40-60 eV region.

2D Graph 1

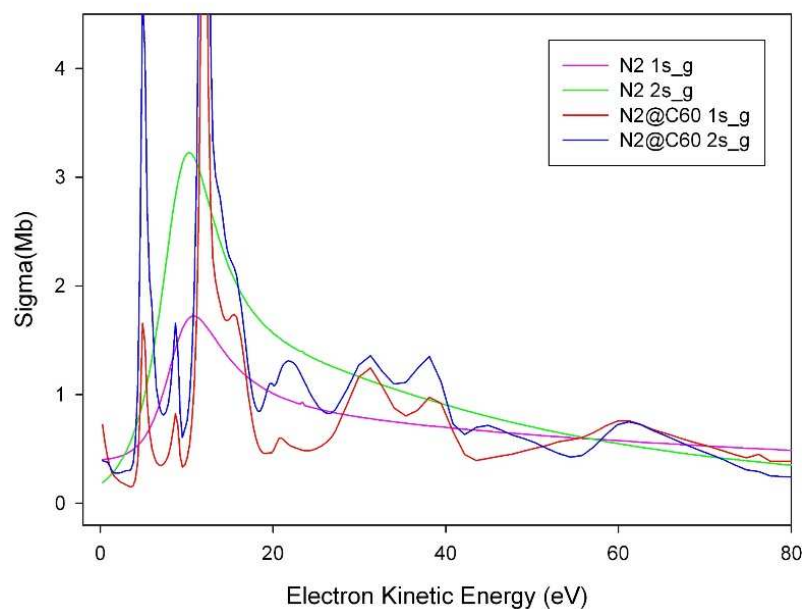


Figure 8. Cross section for the $1\sigma_g$ and $2\sigma_g$ ionization in $N_2@C_{60}$ compared to free N_2 .

The same behavior is observed for β in figure 9, where the two profiles are almost superimposed. It appears that the very different spatial extension of $1\sigma_g$ and $2\sigma_g$, which is reflected in the higher cross section at low energy followed by a faster decay in the latter, has negligible influence on the interaction of the final photoelectron waves, which are influenced by the symmetry and the basic s-type atomic shape common to both initial states.

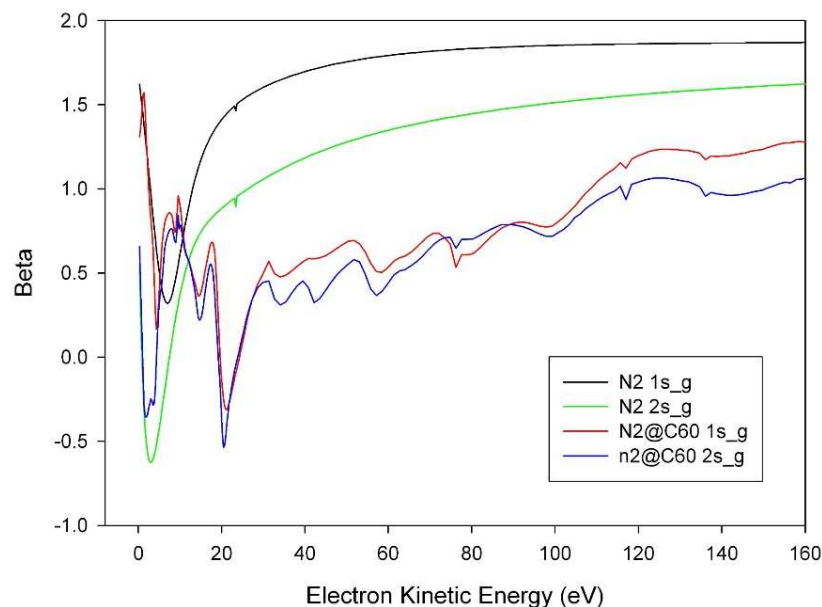


Figure 9. β parameter for $1\sigma_g$ and $2\sigma_g$ photoionization in $N_2@C_{60}$ compared to free N_2 .

IV. Conclusions

Photoionization cross sections and angular distributions for core and inner valence ionization in $N_2@C_{60}$ have been computed at the molecular DFT level and compared with those of free N_2 . A strong modification of free N_2 photoionization parameters has been observed, notably the presence of strong resonances, showing a more complex structure than found in atomic endohedral systems. In particular the interplay of native resonance in the N_2 $1\sigma_g$ channels with the confinement resonances gives rise to a richer structure compared to the $1\sigma_u$ which shows the more regular pattern due to confinement resonances. The interleaving of resonances in the gerade and ungerade channels is observed for the first time, and related to the same phenomenon in free C_{60} . Rather different behavior is observed for the β parameter, where the g/u symmetry is of minor influence. Finally both core $1\sigma_g$ and valence $2\sigma_g$ show a very similar behavior, indicating the dominant effect of orbital shape and minor effect of spatial extent of the orbital.

Acknowledgments

We gratefully acknowledge computer time on the Galileo computer at Cineca, Italy. The work of STM was supported the US Department of Energy, Office of Basic Sciences, Division of Chemical Science, Geosciences and Biosciences under Grant No. DE-FG02-03ER15428.

References

1. Chai Y, Guo T, Jin CM, Haufler R E, Chibante L P F, Fure J, Wang LH, Alford J M, Smalley R E. 1991 Fullerenes with metals inside. *J. Phys. Chem.* **95**, 7564–7568.
2. Saunders M, Cross R J, Jimenez-Vazquez H A, Shimshi R, Khong A. 1996 Noble gas atoms inside fullerenes. *Science* **271**, 1693–1697.
3. Dolmatov V K, Baltenkov A S, Connerade, Manson S T. 2004 Structure and photoionization of confined atoms, *Radiat. Phys. Chem.* **70**,417-433
4. Dolmatov, V K. 2009 Photoionization of Atoms Encaged in Spherical Fullerenes, *Adv. Quantum Chem.* **58**,13–68
5. Deshmukh P C, Jose J, Varma H R, Manson S T, 2021 Electronic structure and dynamics of confined atoms. *Eur. Phys. J. D* in press
6. Komatsu K, Murata M, Murata Y. 2005 Encapsulation of molecular hydrogen in fullerene C₆₀ by organic synthesis. *Science* **307**, 238–240.
7. Kurotobi K, Murata Y. 2011 A single molecule of water encapsulated in fullerene C⁶⁰. *Science* **333**, 613–616.
8. Whitener Jr K E, Frunzi M, Iwamatsu S-I, Murata S, Cross RJ, Saunders M. 2008 Putting ammonia into a chemically opened fullerene. *J. Am. Chem. Soc.* **130**, 13 996–13 999.
9. Whitener Jr K E, Cross R J, Saunders M, Iwamatsu S-I, Murata S, Mizorogi N, Nagase S. 2009 Methane in an open-cage [60] fullerene. *J. Am. Chem. Soc.* **131**, 6338–6339
10. Komatsu K. 2013 Molecular surgical synthesis of H₂@C₆₀: recollections. *Phil. Trans. Roy. Soc A* **371** 20110636.
11. Krachmalnicoff A, Bounds R, Mamone S, Iom S, Concistrè M, Meier B, Kouřil K, Light M E, Johnson M R, Rols S, Anthony J, Horsewill A J, Anna Shugai A, Urmas Nagel U, Rõõm T, Carravetta M, Levitt M H, Whitby R J, 2016 The dipolar endofullerene HF@C₆₀, *Nat. Chem.* **8** 95
12. Connerade J P, Dolmatov V K, Manson S T. 2000 On the Nature and Origin of Confinement Resonances, *J. Phys. B: At. Mol. Opt. Phys.* **33**, 2279-2285
13. Kilcoyne A L D , Aguilar A, Müller A, S. Schippers S, C. Cisneros C, Alna'Washi G, Aryal N B, Baral K K, Esteves D A, Thomas C M, Phaneuf R A. 2010 Confinement Resonances in Photoionization of Xe@C₆₀⁺, *Phys. Rev. Lett.* **105**, 213001
14. Phaneuf R A, Kilcoyne A L D, Aryal N B, Baral K K, Esteves-Macaluso D A, Thomas C M, Hellhund J, Lomsadze R, Gorczyca T W, Balance C P, Manson S T, Hasoglu M F, Schippers S, Müller A. 2013 Probing confinement resonances by photoionizing Xe inside a C⁺₆₀ molecular cage. *Phys. Rev. A* **88**, 053402
15. Hergenahn U, Kugeler O, Rüdell A, Rennie E E, Bradshaw A M. 2001 Symmetry selective observation of the N 1s shape resonance in N₂. *J. Phys. Chem. A* **105** 5704–5708.
16. Stener M, Fronzoni G, Decleva P. 2002 Time dependent density functional study of the symmetry resolved N 1s photoionization in N₂. *Chem. Phys. Lett.* **351**, 469-474
17. Semenov S K, Cherepkov N A, Matsumoto M, Fujiwara K, Ueda, Kukuk E, Tahara F, Sunami T, Yoshida H, Tanaka T, Nakagawa K, Kitajima M, Tanaka H, De Fanis A. 2006 Vibrationally resolved photoionization of the 1σ_g and 1σ_u shells of N₂ molecule. *J. Phys. B: At. Mol. Opt. Phys.* **39** 375–386
18. Liu X J, Cherepkov N A, Semenov S K, Vimberg V, Gel'mukhanov F, Prümper G, Lischke T, Tanaka T, Hoshino M, Tanaka H, and Ueda K. 2006 Young's double-slit experiment using core-level photoemission from N₂: Revisiting Cohen-Fano's two-centre interference phenomenon. *J. Phys. B: At. Mol. Opt. Phys.* **39** 4801–4817.

- 1
- 2
- 3 19. Bachau H, Cormier E, Decleva P, Hansen J E, Martin F. 2001 Applications of B-splines in
- 4 Atomic and Molecular Physics, *Rep. Prog. Phys.* **64**, 1815-1943
- 5 20. Toffoli D, Stener M, Fronzoni G, Decleva P. 2002 Convergence of the Multicenter B-spline
- 6 DFT approach for the continuum. *Chem. Phys.* **276**, 25-43
- 7 21. Ponzi, A Manson S T, Decleva P. 2020 Photoionization of C₆₀: Effects of correlation on
- 8 cross sections and angular distributions of valence subshells. *J. Phys. Chem. A* **124** 108-125
- 9 22. Benning P J, Poirier D M, Troullier N, Martins J L, Weaver J H, Hauñer R E, Chibante L P
- 10 F, Smalley R E. 1991 *Phys. Rev. B* **44**, 1962-1965
- 11 23. Colavita P, De Alti G, Decleva P, Fronzoni G, Stener M. 2001 Theoretical study of the
- 12 valence and core photoemission spectra of C₆₀. *Phys. Chem. Chem. Phys.* **3**, 4481-4487
- 13 24. Decleva P, Toffoli D, Kushawaha R K, MacDonald M, Piancastelli M N, Simon M. Zuin L.
- 14 2016 Interference effects in photoelectron asymmetry parameter (β) trends of C 2s⁻¹ states of
- 15 ethyne, ethene and ethane. *J. Phys. B: At. Mol. Opt. Phys.* **49** 235102
- 16
- 17
- 18
- 19
- 20
- 21
- 22
- 23
- 24
- 25
- 26
- 27
- 28
- 29
- 30
- 31
- 32
- 33
- 34
- 35
- 36
- 37
- 38
- 39
- 40
- 41
- 42
- 43
- 44
- 45
- 46
- 47
- 48
- 49
- 50
- 51
- 52
- 53
- 54
- 55
- 56
- 57
- 58
- 59
- 60